AN EDGE DETECTOR BASED ON WIDE-NARROW MORPHOLOGICAL OPERATIONS OF SATELLITE REMOTE SENSING IMAGES

Makoto KAWAMURA, Toyohashi University of Technology, JAPAN
Yuji TSUJIKO, Fukui National College of Technology, JAPAN
Sanath JAYAMANNA, Toyohashi University of Technology, JAPAN

Commission III, Working Group 3

KEY WORDS: Remote_Sensing, Classification, Extraction, Algorithm, Edge, Landsat

ABSTRACT

In a classification of satellite remote sensing data, spectral distribution in a feature space is usually used. However, MIXELs at class boundaries cause miss-classification results. To solve this problem many researchers have carried out increasing the feature space dimensions by giving additional information. In this study, we describes the method creating additional information mentioned above. In particular, a new Wide-Narrow Morphological Edge Detection (WNED) algorithm to make edge information is introduced. WNED differs from previous morphological edge detectors in that it manipulates two conventional minimum-based operations in the target domain at the same time. As the results of a case study for Landsat TM data it is found that WNED algorithm is effective to extract edge information clearly and it can control the detection of the spurious edge information.

1. INTRODUCTION

Remote sensing technology has contributed in assisting to make accurate maps timely, widely and economically. A large number of studies have introduced the effectiveness of satellite remote sensing data and its applicabilities for the monitoring. In the land cover classification, however, mixed pixels (mixel) which are laid among some categories produce the miss-classification outpts. To extract or to avoid these pixels, many researchers have tried to detect edge pixels using conventional segmentation methods such as convolutional filterings. Recently, there are some cases using mathematical morphology to execute the segmentation (Kawamura, 1994 and 1995)). This study also describes the segmentation method in terms of edge detection to improve the classification accuracy using mathematical morphology. In particular, a new algorithm to make accurate and clear edge information is introduced.

Theoretical background of mathematical morphology was established at the Centre de Morphologie Mathematique in France, in the mid 1970's (Matheron, 1975) and extended to application for image processing (Haralick, 1987). It is also well-known that image shape features such as edges, fillets, holes and skeletons can be obtained by combining morphological fundamental operations and structuring elements. In this study, the combination of morphological fundamental operations and structuring elements is focused.

2. MORPHOLOGICAL OPERATION

Morphological operations are classified in a binary morphology and a gray-scale morphology. Usually satellite remote sensing data are given as gray-scale image. Therefore this analysis describes the gray-scale morphological operations. The gray-scale morphological operations can be defined as follows. Let f(x) and k(x) be 1-dimesional gray-tone functions of coordinate x, where f(x) is the original remote sensing image, and k(x) is the operator (filter) called structuring element. Let E represent Euclidean space. Then $f:F\rightarrow E$ and $k:K\rightarrow E$. The dilation and the erosion operations are defined as follows:

$$\text{dilation}: (f\oplus k)(x)=\max\{f(x-z)+k(z)\}\equiv d(x) \quad \forall z\in K,\ x-z\in F \tag{1}$$

$$\text{erosion}: (f\ominus k)(x)=\min\{f(x+z)-k(z)\}\equiv e(x). \quad \forall z\in K,\ x+z\in F \tag{2}$$

The opening and closing operations can be defined in terms of dilation and erosion operations as follows:

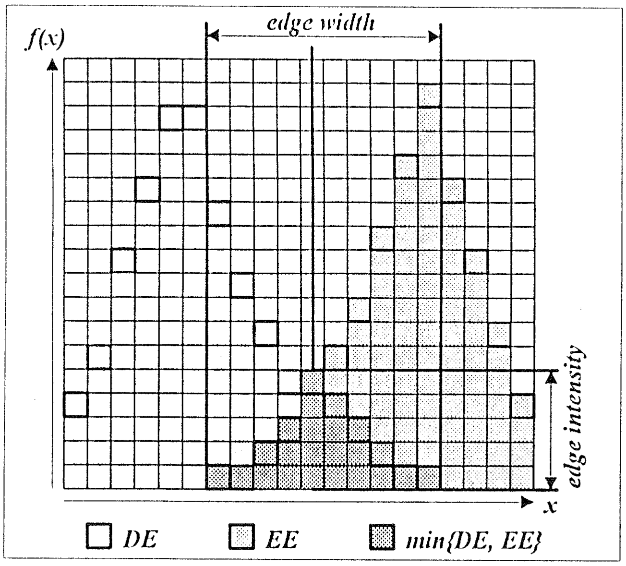

Figure 1 Concepts of dilation- erosion-residual edge
(DE:dilation-residual edge, EE:erosion-residual edge)

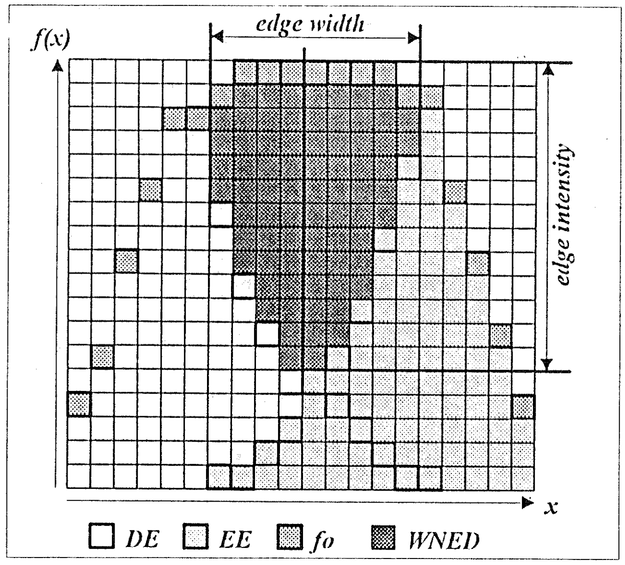

Figure 2 Concept of WNED

$$\text{opening}: o(x)=((f\ominus k)\oplus k)(x) \tag{3}$$

$$\text{closing}: c(x)=((f\oplus k)\ominus k)(x). \tag{4}$$

Since the erosion in opening is firstly computed, it has a feature that deletes small noises. Similarly closing can extract the small gradients by calculating dilation in the first step.

3. MORPHOLOGICAL EDGE DETECTION

Conventional simple morphological edge detector is the dilation-residual edge image (dilation-type) is as follows:

$$\text{dilation-type}: DE(x)=d(x)-f(x) \quad \text{or} \quad DE'(x)=c(x)-f(x) \tag{5}$$

Similarly the erosion-residual edge image (erosion-type) is as follows:

$$\text{erosion-type}: EE(x)=f(x)-e(x) \quad \text{or} \quad EE'(x)=f(x)-o(x) \tag{6}$$

Even though DE and EE are simple and robust, they are not effective for images which have extremely noisy pixels. In the case of using these detectors, the outputs may introduce spurious edges. For the original image, DE extracts higher (value) side edges and EE extracts lower side edges.

Figure 1 shows concepts of edge detection for DE and EE. As shown in the figure, the extreme points of overlapped pixels are considered the real edge pixels. To detect the real edge pixels the minimization of dilation- erosion-residual edge pixels are introduced. Lee et al. designed BMM (Blur Minimization Morphological) operator (Lee, 1987) and Feehs et al. showed ATM (Alpha Trimmed Multidimensional Morphological) edge detector (Feehs, 1987). BMM is shown as follows:

$$BMM(x)=\min\{fa(x)-e(x),\ d(x)-fa(x)\} \tag{7}$$

where fa(x) is a blurred image. BMM operator blurs the original image by averaging the pixel values spanned by the structuring element. Dilation and erosion image for blurred image are computed in the first step. Erosion- and dilation-residual images are created using these images. The edge intensity at coordinate x is given by the minimum of the dilation-residual and erosion-residual images. ATM is shown as follows:

$$ATM(x)=\min\{o(x)-e(x),\ d(x)-c(x)\} \tag{8}$$

where the original image for dilation and erosion is initially blurred.

BMM has been proven to perform better than the spatial-based and differential-based edge detectors and ATM has also proven statistically that performs better than BMM. These operators, however, are unable to extract the weak gradients. For increased structuring element sizes, weak gradients are extracted, along with other spurious edge pixels which are difficult to isolate.

To improve the problem, we show WNED (Wide-Narrow Edge Detection) algorithm which is combined two minimization (maximization) algorithm. As shown in Figure 2 the edge intensity of WNED is larger than the minimum based edge detectors'. If the structuring element sizes are increased, minimum based operators such as BMM and ATM extract the weak gradients. In contrast to such operators, WNED can separate the edge pixels and the other pixels. This possibly could be because the edge intensity of WNED is more significant than the minimum based edge detectors. Symbolically WNED is written as:

Figure 3 Original image (f(x))

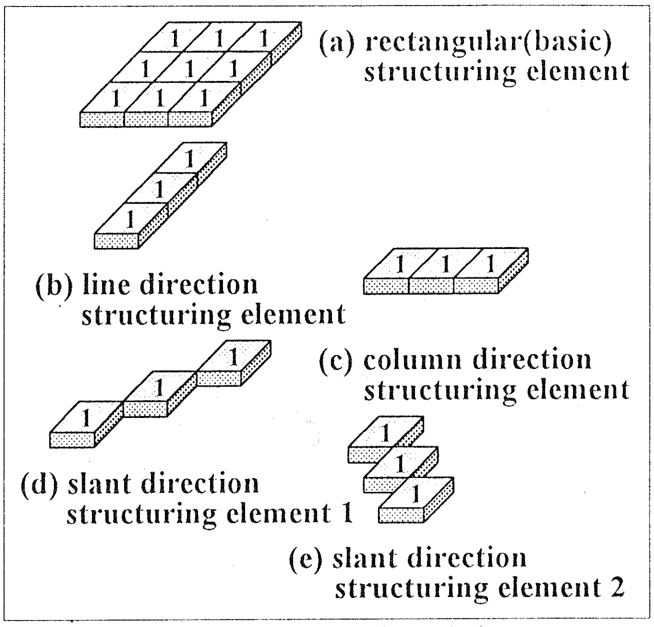

Figure 4 Structuring elements (k(x))

$$\text{WNED}(x)=fo-\max\{DE, EE\} \qquad (9)$$

where fo is output of wide range detection. In this study, we use:

$$fo=\max\{d(x)-o(x), c(x)-e(x)\}. \qquad (10)$$

4. CASE STUDY

4.1 Data

NVI image given by the near infrared band (band 4) and the visible image band (band 3) of Landsat TM purchased from RESTEC, JAPAN is used as the original image. It is for path=109 and row=36 which covers the center of Nagoya, Japan. Particularly 100× 100 pixels surroundings of Kiso river are selected. Figure 3 shows the original image. The target edge pixels are boundaries of land and river.

4.2 Selection of structuring element

There are many types of structuring elements in the previous works (Maragos, 1987). This analysis provides four types of structuring elements as shown in Figure 4. In this paper, the cases applying 3×3 (Figure 4(a))are introduced.

4.3 Results

Figure 5 all show the results by morphological edge detectors. (a) and (b) show the results of applying the DE and EE with structuring elements (k(x)) of size 3× 3 respectively. Many different edge intensities are found in these two images. (c) in the same figure show the minimum of DE and EE which is a similar mannar to BMM and ATM. In the figure, many undesiable pixels are extracted. In the case of increasing the structuring element sizes, the extracted pixels of (c) were expanded according to the expansion of structuring elements. WNED outputs are shown in Figure 5(d). In comparison with other outputs, it is found that WNED can extract edge clearly and control the spurious edge detection. For increasing structuring element sizes, WNED did not expand the edge pixels comparing with the minimum based edge detection.

5. CONCLUSION

It is found that WNED algorithm is effective in case of detecting rapid change of gray-tone functions such as boundaries of the river and it can control the spurious edge detection. Proposed algorithm is also useful for the unknown target, because it doesn't expand the edge pixels regardless of increasing structuring element sizes.
By using this method it is considered that it is able to use monitorings the disaster such as a flood.

REFERENCES

Feehs R. and Ace G., 1987. Multidimensional edge detection. Proc. SPIE, Visual Commun. Image Processing II, Vol.845, pp. 285-292.

Haralick R., Sternberg S. and Zhuang X., 1987. Image analysis using mathematical morphology. IEEE Trans. Pattern Anal. Machine Intell., Vol.PATM-9.

Kawamura M. and TSUJIKO Y., 1994. Multispectral classification of Landsat TM data using a cooperative learning neural network. Proc. of IGARSS '94, Vol.2, pp.508-512.

Kawamura M. and TSUJIKO Y., 1995. An approach to geographic pattern recognition using mathematical morphology. Proc. of IGARSS '95.

Lee J., Haralick R. and Shapiro L., 1987. Morphological edge detection. IEEE J. Robotics Automation, Vol.RA-3.

Maragos P. and Schafer R. W., 1987a. Morphological filters-Part I. IEEE Trans. Acoust. Speech Signal Processing, Vol.ASSP-35, No.8, 1153-1169.

Maragos P. and Schafer R. W., 1987b. Morphological filters-Part II. IEEE Trans. Acoust. Speech Signal Processing, Vol.ASSP-35, No.8, 1170-1185.

Matheron G., 1975. Random Sets and Integral Geometry. New York, Wiley.

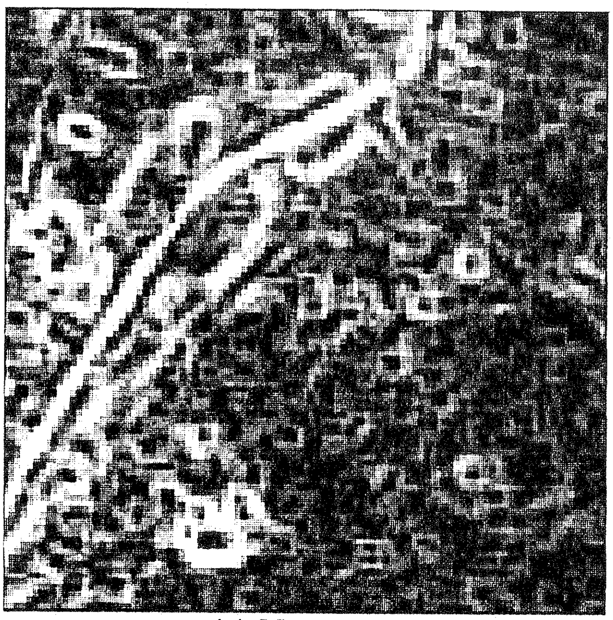

(a) DE

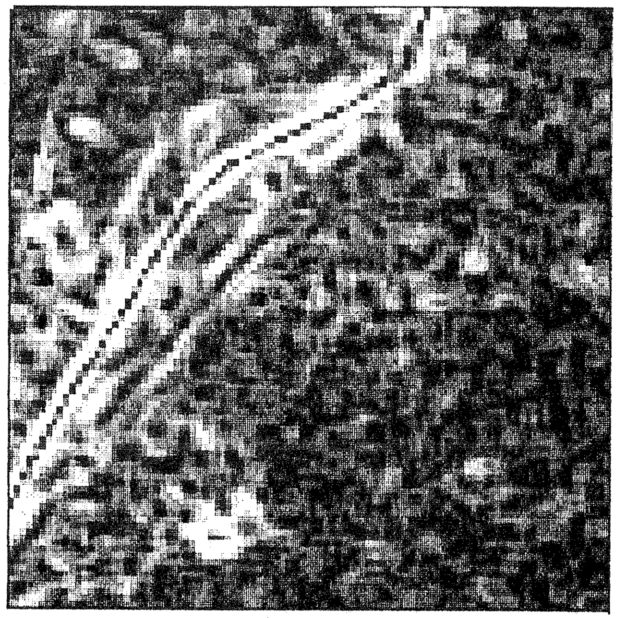

(b) EE

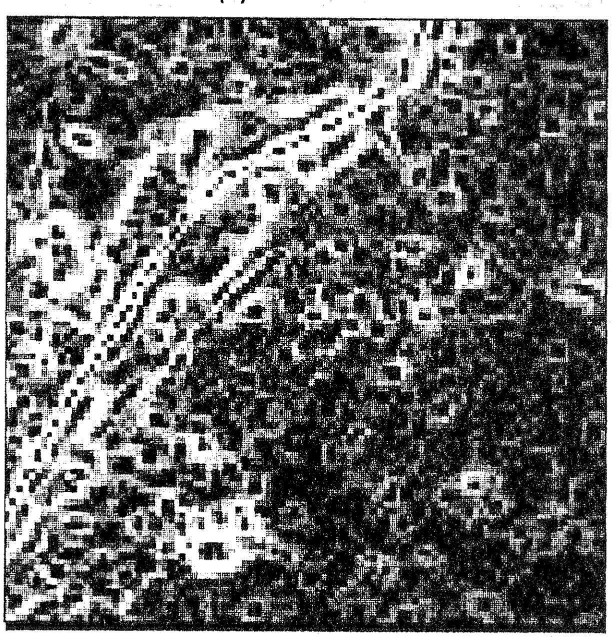

(c) min{DE, EE}

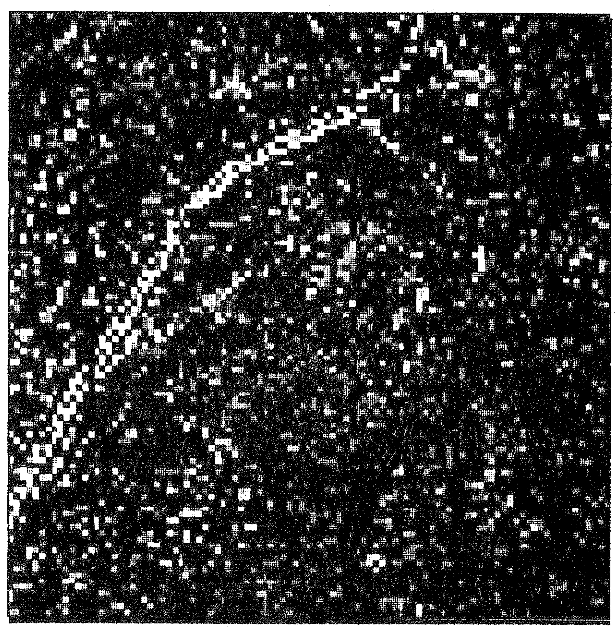

(d) WNED

Figure 5 Results